Development of Soft X-Ray Flat-Field Holographic Gratings for the Measurement of *K* Emission Spectrum of Li

Takashi Imazono,[1] Masato Koike,[1] Tetsuya Kawachi,[1] Noboru Hasegawa,[1] Masaru Koeda,[2] Tetsuya Nagano,[2] Hiroyuki Sasai,[2] Yuki Oue,[2] Zeno Yonezawa,[2] Satoshi Kuramoto,[2] Masami Terauchi,[3] Hideyuki Takahashi,[4] Nobuo Handa,[4] Takanori Murano,[4] Kazuo Sano[5]

1) *Quantum Beam Science Directorate, Japan Atomic Energy Agency (JAEA), 8-1-7 Umemidai, Kizugawa, Kyoto 619-0215 Japan*

2) *Device Department, Shimadzu Corp., 1 Nishinokyo-Kuwabara-cho, Nakagyo-ku, Kyoto 604-8511 Japan*

3) *Institute of Multidisciplinary Research for Advanced Materials, Tohoku University, 2-1-1 Katahira, Aoba-ku, Sendai 980-8577 Japan*

4) *EO Peripheral Components Business Unit, JEOL Ltd., 3-1-2 Musashino, Akishima, Tokyo 196-8558 Japan*

5) *Shimadzu Emit Co. Ltd., 2-5-23 Kitahama, Chuo-ku, Osaka 541-0041 Japan*

Abstract

We have developed a wavelength-dispersive soft x-ray spectrograph covering an energy region of 50-4000 eV to attach to a conventional electron microscope. The energy range was properly divided into four ranges of 50-200 eV, 155-350 eV, 300-2200 eV, and 2000-4000 eV, and a versatile spectrograph equipped with interchangeable multiple gratings optimized in the respective energy ranges has been developed. In particular, the grating that covers the 50-200 eV range can be used for the measurement of the *K* emission spectrum (~55 eV) of lithium. The diffraction efficiency evaluated by synchrotron radiation and resolving power measured by laser produced plasma sources are over 5% and in excess of 700, respectively. The *K* emission spectrum of metallic Li with high spectral resolution has been successfully observed with the spectrograph attached to a transmission electron microscope.

1. Introduction

In miniaturization of semiconductor devices and new functional materials, it is extremely important to perform not only structural and elemental analyses but also to investigate chemical properties in the nanometer scale. In the observation of materials in nanometer-scale spatial resolution, electron microscopies (EM's) such as scanning and transmission electron microscopy (SEM/TEM) are utilized for evaluating the structural and elemental analyses in a variety of fields. Chemical properties strongly depend on electronic structure of valence electrons (bonding electrons). Therefore, it is a very attractive to introduce a spectroscopic method for the study of valence band states in nanometer scale into EM's.

Electron energy-loss spectroscopy (EELS) based on TEM is effective technique for analyzing the electronic structure in identified nanometer areas. EELS spectrum gives the information on interband transition and plasmon energies in the valence excitation region and the partial density of state (DOS) of the unoccupied electronic structure (conduction band: CB) and composition in the inner-shell excitation region, which is equivalent information to x-ray absorption fine structure (XAFS). On the contrary, the information on the occupied electronic structure (valence band: VB) of a material can be obtained using soft x-ray emission spectroscopy (SXES). The soft x-ray emission (SXE) spectrum reflects a partial DOS of the VB state.

A conventional electron probe microanalysis (EPMA) instrument is typically based on a wavelength or energy dispersive x-ray spectroscopy (WDS or EDS). A WDS instrument needs a wavelength scanning mechanism due to narrow detection angle of a dispersive crystal. EDS generally has a wide acceptable range without mechanical movement but suffers inferior resolving power compared to WDS. Also the elements which can be detected by commercial WDS and EDS instruments are restricted to a larger atomic number than boron (B). Consequently the *K* emission spectrum of lithium, which is an important element in the development of rechargeable batteries, is difficult to be measured by conventional instruments.

The B-*K* emission spectrum of boron nitride in the nanometer region was measured at high resolving power of 300 at ~190 eV for the first time [1] by a wavelength dispersive spectrograph equipped with a mechanically-ruled varied-line-spacing (VLS) flat-field diffraction grating [2] attached to a conventional transmission electron microscope (TEM). This technique has a possibility to observe weak SXE spectrum based on TEM and makes it possible to overcome some difficulties in WDS and EDS as well as obtain the SXE spectra with high efficiency and resolution in the nanometer area. Hence, it is shown that SXES and EELS based on TEM can comprehensively analyze the electronic structures associated with

both the VB and CB states along with the structural and elemental properties of the specified material [3].

Our purpose is to establish TEM-SXES in an energy region of 50-4000 eV by use of a flat-field grating spectrograph, in which various characteristic x-rays of functional materials would be observed, e.g., Li-*K* (55 eV) and C-*K* (277 eV) emission spectra of secondary battery electrode materials, B-*K* (180 eV) and Co-*L* (780 eV) of steel materials, Pt-*M* (2050 eV), Au-*M* (2123 eV), and Pd-*L* (2838 eV) of catalytic materials, and In-*L* (3287 eV) and Te-*L* (3769 eV) of chalcogen compound as a solar cell and fluorescence materials. Unfortunately, it is impossible to cover the 50-4000 eV range using a standard flat-field spectrograph, which is equipped with a single VLS grating with an effective groove density of 1/1200 mm and at an angle of incidence of 87.0° measured from the grating normal [2]. As the solution of this problem, we have properly divided the 50-4000 eV range into four ranges as (1) 50-200 eV (24.8-6.2 nm), (2) 155-350 eV (8.0-3.5 nm), (3) 300-2200 eV (4.13-0.56 nm), and (4) 2000-4000 eV (0.62-0.31 nm), and to develop a versatile spectrograph which can accommodate interchangeable multiple gratings optimized in the respective energy ranges. In this case, it is important to be able to alternate the optical systems without complicated aliment in the practical use.

In the 50-2000 eV range, it would be possible to obtain high diffraction efficiency even a metallic single layer of Au, Pt, Ni, etc deposited on the grating surface, however, such layers are no longer practicable in the energy above 2000 eV. Thus a multilayer coating in place of a single layer should be applied to enhance the diffraction efficiency [4, 5].

In this paper, firstly we describe the design of a versatile flat-field spectrograph that can accommodate four holographic VLS gratings briefly, and state the design, fabrication, and evaluation of the grating that covers the lowest energy range of 50-200 eV. Then we describe the performance of the fabricated four types of gratings, i.e., laminar and blazed types master (LM and BM) gratings and the respective replica (LR and BR) gratings. The absolute diffraction efficiencies of the gratings of LM, LR, BM, and BR are measured in the 50-250 eV range using synchrotron radiation (SR) as well as their energy resolution has been determined in the vicinity of 50 eV using laser produced plasma (LPP) light sources. Finally, the *K* emission spectrum of metallic Li obtained by the TEM-SXES experiment is shown.

2. Design and fabrication of laminar and blazed holographic gratings

Four holographic gratings have been optimized for the energy ranges of 50-200 eV, 155-350 eV, 300-2200 eV, and 2000-4000 eV, respectively, so as to develop a versatile

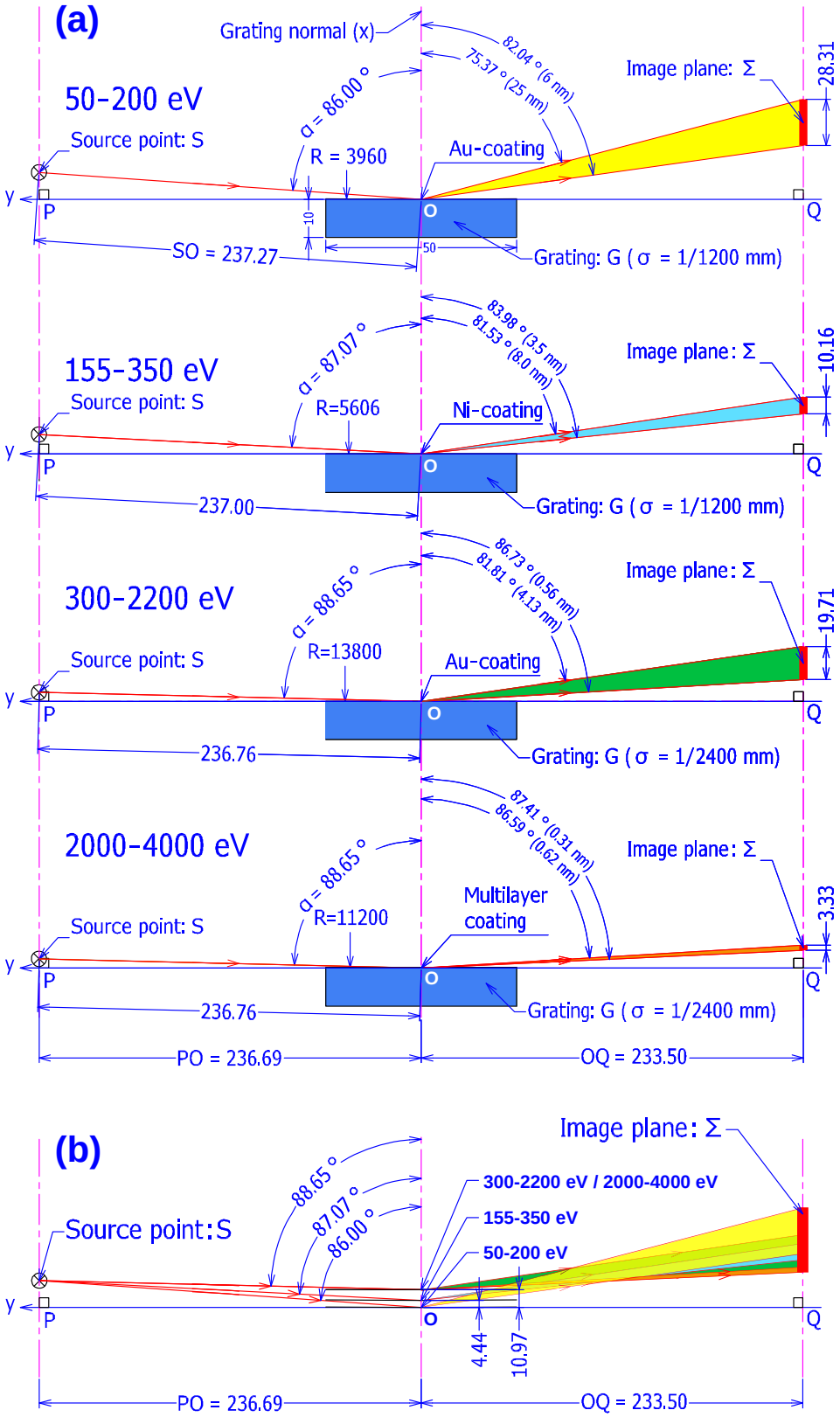

Fig. 1 Schematics of the designed flat-field spectrograph (a) and the spectrograph shown as being compatible with all gratings by the offset of the grating center parallel to the *x* direction (b). The distances of PO and OQ, and the direction of grating normal are common in the spectrograph.

Table 1. Details of the parameters for the holographic VLS gratings optimized for the energy ranges of 50-200 eV, 155-350 eV, 300-2200 eV, and 2000-4000 eV, respectively. E is energy range, λ is wavelength range, α is the angle of incidence, SO is the distance between the source point and origin O, PO is the projection of SO onto the y-axis, OQ is the distance between the point Q where the image plane Σ intersects the y-axis and origin, Δ is the offset from O, X_Σ is the spectral length of image plane, and G.S. is groove shape, σ is the effective grating constant, R is the radius of curvature, h is the groove depth, D.R. is the duty ratio (land/grating constant), θ_B is blaze angle, and λ_B is blaze wavelength, of the grating.

E/eV	50-200		155-350	300-2200	2000-4000
λ/nm	25-6		8.0-3.5	4.13-0.56	0.62-0.33
α/deg	86.00		87.07	88.65	88.65
SO/mm	237.27		237.00	236.76	236.76
PO/mm	236.69 (common parameter)				
OQ/mm	233.50 (common parameter)				
Δ/mm	0		4.44	10.97	10.97
X_Σ/mm	28.31		10.16	19.71	3.33
G.S.	Laminar	Blazed	Laminar	Laminar	Laminar
σ/mm	1/1200		1/1200	1/2400	1/2400
R/mm	3960		5606	13800	11200
h/nm	20	−	16	5	2.8
D.R.	0.3	−	0.3	0.3	0.5
θ_B/deg	−	3.0	−	−	−
λ_B/nm	−	10.0	−	−	−
Coating	Au		Ni	Au	Multilayer
$x \times y \times z$/mm^3	$10 \times 50 \times 30$				

flat-filed spectrograph which accommodates interchangeably from the viewpoint of practical use, the spectrograph should be designed to be compatible with four gratings [6]. A solution for this design concept is to fix the positions of a light source, the image plane, and the direction of the grating normal in the optical parameters of the spectrograph equipped with each grating. Figure 1(a) shows a schematic of the designed flat-field spectrographs equipped with the four gratings, of which the major design parameters are listed in Table 1. Three optical parameters of the distances PO and OQ, and the direction of the grating normal are designed to be common among four spectrographs. It means that α changes by changing the position of the grating. Thus, the optical system is interchangeable with all the gratings. The design goals of resolution have been set as 300 at Li-K (~55 eV) emission spectrum, 1000 at B-K (~180 eV), 300 at Co-L (~780 eV), and 100 at Te-L (~3800

eV). The details of fabrication and performance of all gratings would be reported in another paper [7]. We describe only the grating which covers the lowest energy range of 50-200 eV in this paper.

We used a combination of an aspheric wavefront resulting from the reflection of a spherical wavefront from a spherical mirror and a spherical wavefront to record a holographic groove pattern [8]. Assuming the effective grating constant σ = 1/1200 mm and recording laser wavelength λ_0 = 441.6 nm, the optimized recording parameters determined by means of an analytical design method are R_1 = 599.13 mm, p_C = 347.839 mm, q_C = 425.000 mm, γ = −8.412°, η_C = −33.508°, r_D = 583.948 mm, and δ = 22.558° (see Fig. 2) [9, 10]. Then groove number n is expressed by a power series of the coordinates P(0, w, l) on the nth grooves as follows: $n_{20} = -1.054 \times 10^{-4}$ mm^{-1}, $n_{02} = -8.205 \times 10^{-4}$ mm^{-1}, $n_{30} = -4.993 \times 10^{-7}$ mm^{-2}, $n_{12} = 2.935 \times 10^{-6}$ mm^{-2}, $n_{40} = -1.026 \times 10^{-5}$ mm^{-3}, $n_{22} = -2.836 \times 10^{-7}$ mm^{-3}, and $n_{04} = -3.351 \times 10^{-8}$ mm^{-3}.

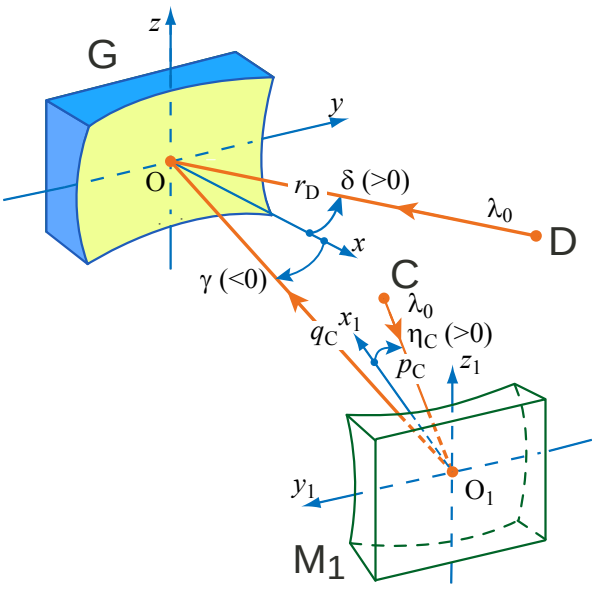

Fig. 2 Schematic of the aspheric wavefront recording optics.

Figure 3 shows the imaging property of the spectrograph evaluated by means of ray tracing. We assumed that the entrance slit was a self-luminous source having dimensions of 2 μm × 2 μm, the grating had a ruled area of 46 mm (W) × 26 mm (H), and a vertical aperture having a 20-mm height in front of the image plane. The spot diagrams and line profiles constructed with 500 rays for three wavelengths of λ and $\lambda \pm \lambda/100$. The pixel size of commercial CCD's which are frequently used for these kinds of spectrographs is 13-20 μm. It corresponds to the resolving power of 200-300 at 6 nm and 800-1200 at 25 nm. It is concluded that the resolution of the spectrograph is estimated

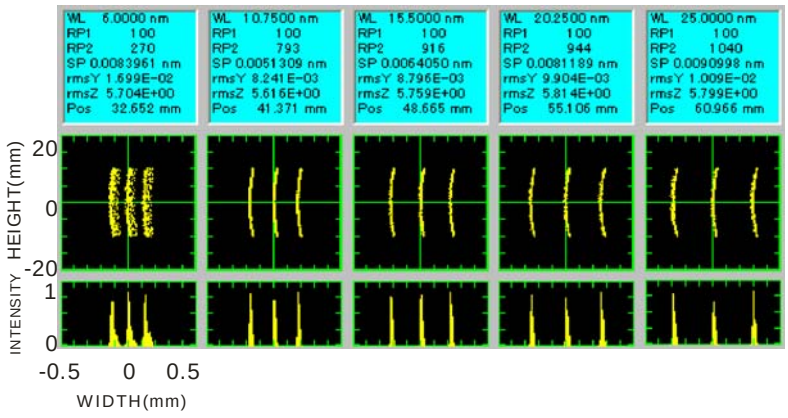

Fig. 3 Spot diagrams and line profiles constructed by ray-tracing.

Table 2 List of fabricated laminar and blazed types gratings.

Groove shape	Series	Type	Notation	Duty ratio	Groove depth (nm)	Blaze angle (°)
Laminar	311	Master	M311	0.27	18.5	-
	312	Master	M312	0.24	19.5	-
	313	Master	M313	0.24	20.5	-
	313	Replica	R3130103	0.27	22.5	-
	313	Replica	R3130201	0.25	22.5	-
	313	Replica	R3130202	0.26	23	-
	314	Master	M314	0.25	20.5	-
	314	Replica	R3140201	0.24	22	-
Blazed	3	Master	M3	-	-	2.9
	3	Replica	R30101	-	-	2.9
	4	Master	M4	-	-	4.8

to be over or comparable to that dominated by the detector.

The laminar and blazed master gratings and the respective replica gratings were fabricated at Shimadzu Corp. For the recording of the groove pattern use was made of the recording system shown in Fig. 2. The substrates of master gratings were made of a borosilicate crown glass (BK7) with a roughness of ~0.3 nm rms. The interference pattern of two laser beams was recorded in a photoresist layer coated on the grating substrate. The laminar or blazed grooves were formed into the substrate by a reactive ion etching process, and then Au coating of 50-100 nm thick was deposited by a conventional vacuum evaporation method. The replica gratings were fabricated from the respective master gratings. A part of fabricated laminar type master (LM) and their replica (LR) gratings and blazed type master (BM) and its replica (BR) gratings were listed in Table 2 with the measured parameters related to the groove shape.

Figure 4 shows calculated absolute diffraction efficiencies of the zero-, first-, second-, and third- orders for LM and BM at the angle of incidence of 86.00° in the wavelength of 5-25 nm. The first order diffraction efficiency curve of LM shows the peak at around 8.5 nm. The second order diffraction efficiency is restricted compared to the first one, which is a typical characterization of laminar type gratings. In the case of BM, the first order diffraction efficiency curve shows the peak at the blaze wavelength of 10 nm and is higher than that of LM in the whole wavelength range. Since the second order diffraction efficiency is also high, the use of which is available for a high resolution measurement.

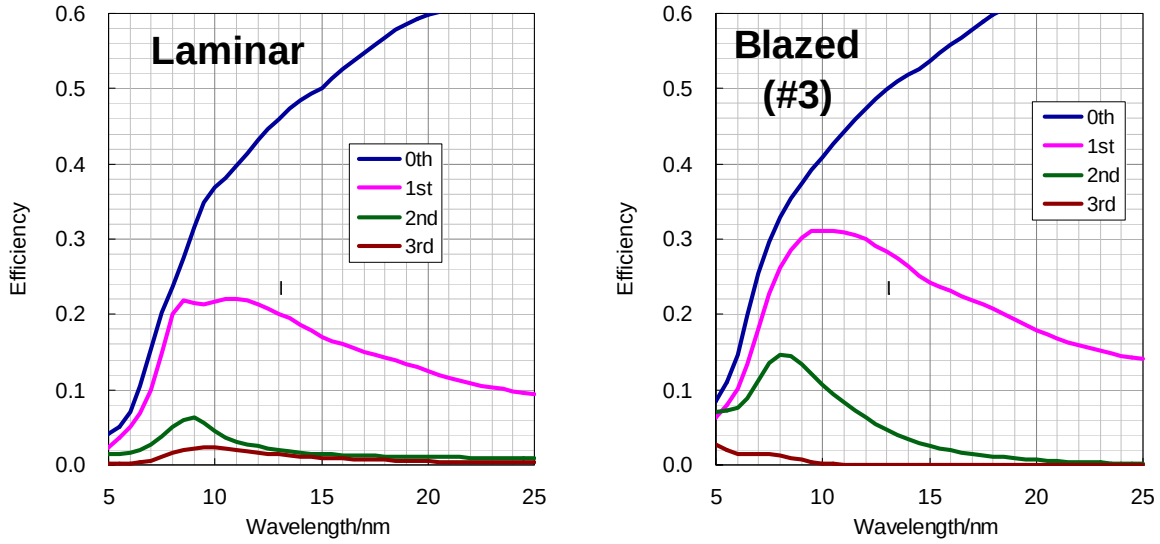

(a) LM (b) BM

Fig. 4. Calculated absolute diffraction efficiencies of the zero-, first-, second-, and third- orders for M313 as the laminar type master (LM) grating (a) and M3 as the blazed master (BM) grating (b) at 86.00° in the wavelength of 5-25 nm.

3. Absolute diffraction efficiency in the 50-200 eV range

The absolute diffraction efficiencies of four types of gratings of LM, LR, BM, and BR were measured using SR at a soft x-ray beamline (BL-11) [11] of SR Center, Ritsumeikan University [12]. This beamline provides soft x-rays in the energy range between 50 eV and 1800 eV by two types of grazing incidence Monk-Gillieson (M-G) monochromators [13, 14]. A conventional M-G monochromator equipped with a laminar-type holographic VLS plane grating of 300 lines/mm was chosen and the incident energy was scanned from 50 eV to 250 eV, in which the resolving power was a few hundreds. Thin films of C, B, Si, and Al with the thicknesses of ~0.5 μm were used to reduce unwanted higher order lights included in the incident light. The size of the incoming beam was approximated to be ~0.5 mm in diameter at the sample in a reflecto-diffractometer installed in the end station of BL-11, which was evaluated by visible light (the zero-th order light) from the monochromator.

Figure 5 shows the absolute diffraction efficiencies of all gratings listed in Table 2 at the angle of incidence of 86.00° in the energy region of 50-250 eV. The zero-, first, and second-orders diffraction efficiencies of laminar type gratings are shown in Figs. 5(a)-(h). In the cases of the blazed type gratings they are shown in Figs. 5(i)-(k), the third-order diffraction efficiencies have also been measured. The measured diffraction efficiencies are in good agreement with the respective calculation curves, shown in Fig. 4. The diffraction

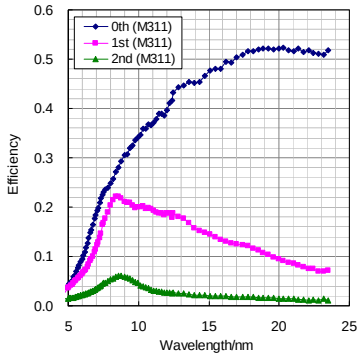

(a) M311

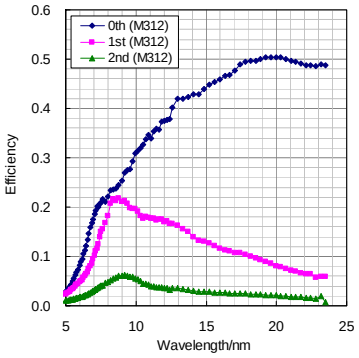

(b) M312

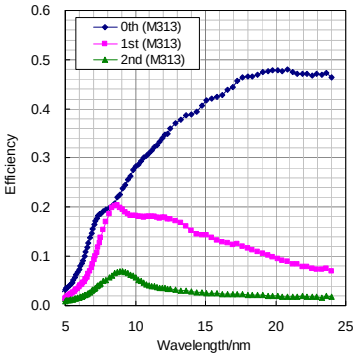

(c) M313

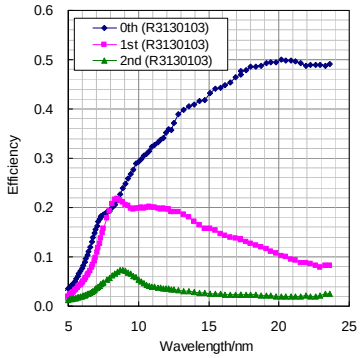

(d) R3130103

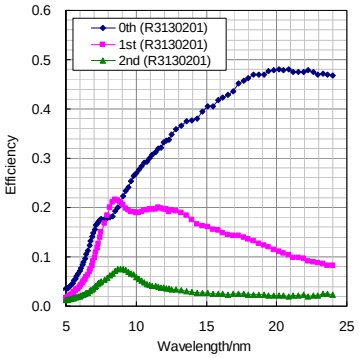

(e) R3130201

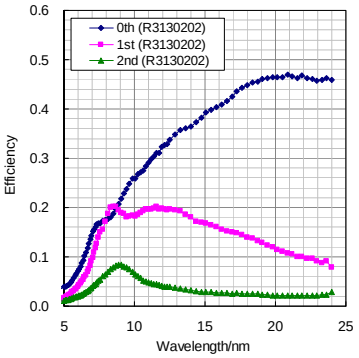

(f) R3130202

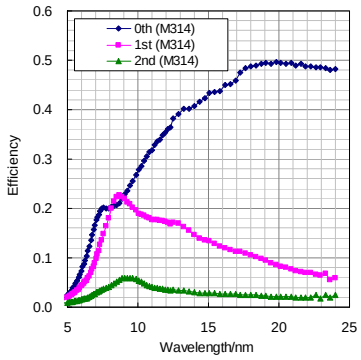

(g) M314

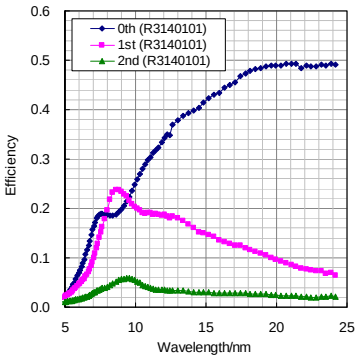

(h)R3140101

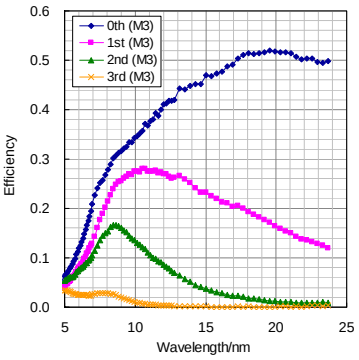

(i) M3

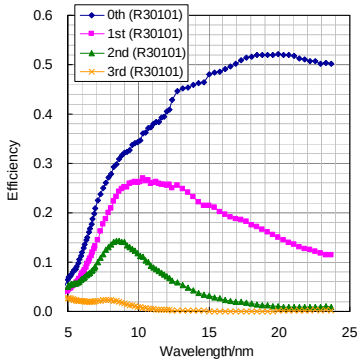

(j) R30101

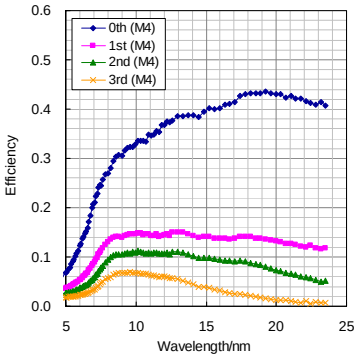

(k) M4

Fig. 5. Absolute diffraction efficiencies of the zero-, first-, and second- order lights for all gratings.

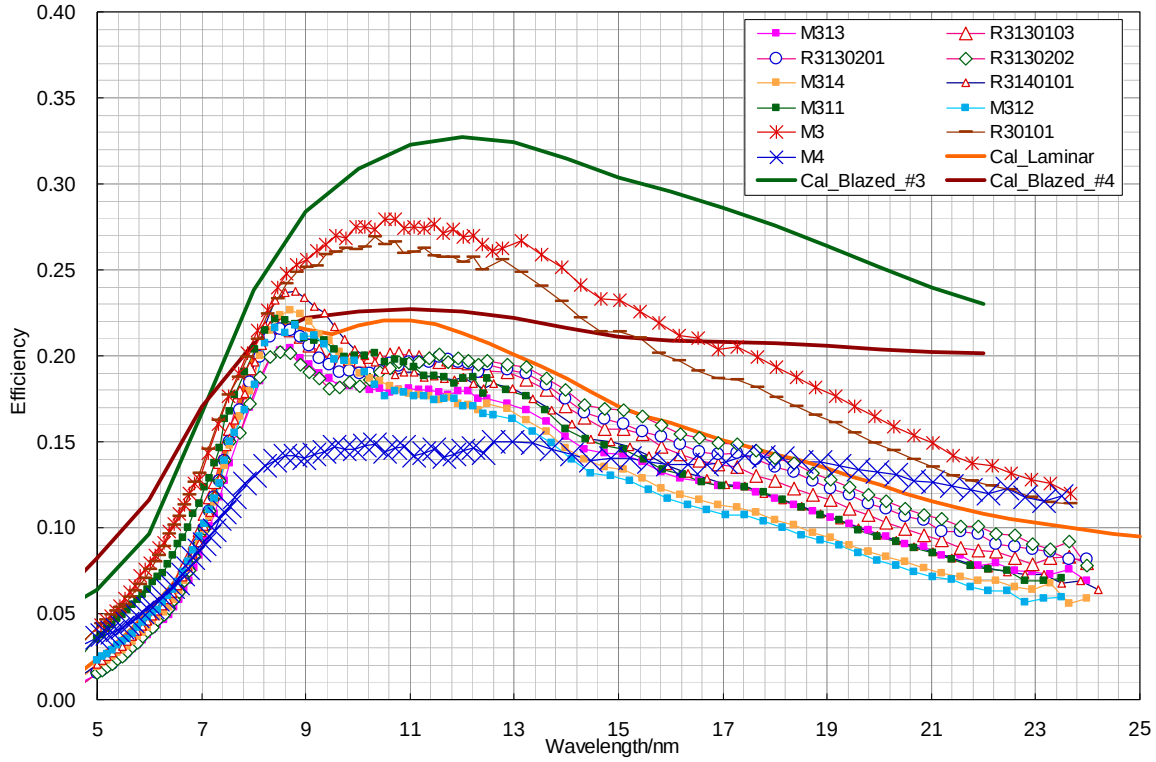

Fig. 6 Comparison of measured and calculated first order diffraction efficiencies of the LM, LR, BM, and BR gratings. Solid lines are the calculated curves.

efficiencies of the first order lights for the laminar type gratings (or blazed type gratings) are in excess of 5% (or 10%) at the energy of Li-*K* emission line (~24 nm). Besides, the second order diffraction efficiencies of blazed gratings are relatively high. It is therefore helpful for the improvement of the energy resolution of two times higher if taking advantage of the second order light. Furthermore, it is found that the efficiencies of the replica gratings are almost comparable to those of the respective master gratings.

For the comparisons of the measured first order diffraction efficiencies of all gratings are shown in Fig. 6. The BM grating of M3 shows the best performance with the maximum of 28% in the vicinity of λ_B = 10 nm, and its replica grating of R30101 is the second place. It was also shown experimentally that the efficiencies of the blazed gratings, i.e., M3 and R30101, with the small blaze angle of ~3°, are superior to those of the laminar gratings in the whole measured region.

4. Resolving power in the vicinity of 50 eV

Resolving power measurements of the gratings were carried out using leaser produced plasma (LPP) sources excited by a Ti:sapphire laser system (ALPHA 10, Thales laser Co. Ltd.) at JAEA. This laser system provided an 800-nm laser pulse of 60 mJ in energy and for

the duration of 80 fs at a 10-Hz repetition rate. Helium gas was irradiated at an intensity of 4×10^{16} W/cm^2. Energetic electrons were generated from the laser-plasma interaction, resulting in bremsstrahlung and the characteristic emission lines associated with the Lyman series of helium being produced [15]. The reason why Lyman series of helium were used is close to the *K* emission spectrum of lithium (~55 eV) [16]. The light source size was estimated to be a 50-μm in diameter. Soft x-rays from the plasma were filtered with an Al-foil of 0.8 μm thickness to remove the bremsstrahlung component. After then filtered soft x-rays were collected and focused with the prefocusing toroidal mirror on the entrance slit having a size of 60 μm × 10 mm meridionally and image plane sagitttally. The use was made of a CCD imaging detector (Princeton Instruments; PIXIS-XO: 2048B; pixel size: 13.5 μm ×13.5 μm; number of pixels: 2048 × 2048). The grating was set at the angle of incidence of 86.00°. From the angular dispersion and focal length of the spectrograph, and the pixel size of the CCD used, the reciprocal line dispersion has been estimated to be 0.8513 nm/mm, i.e., 0.0115 nm/pixel, at He II Ly$_\beta$ (25.632 nm). It corresponds to the resolving power of ~2200 and should be higher than the energy resolution goal and that estimated from the result of ray-tracing. Thus, it indicates that the energy resolution of the spectrograph equipped with the test grating can be properly evaluated.

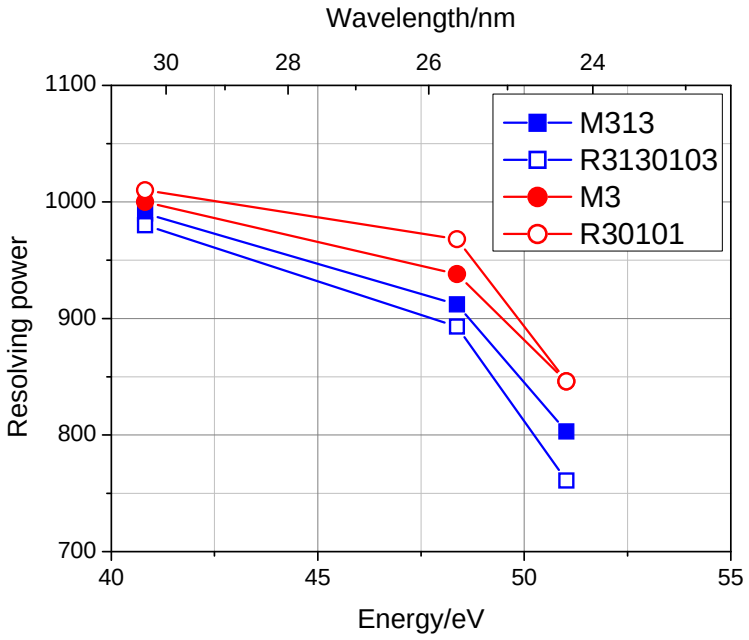

Fig.7. Resolving powers of LM (M313), LR (R3130103), BM (M3), and BR(M30101) gratings evaluated by LPP sources in the vicinity of 50 eV.

The plots of resolving power at the Lyman lines are shown in Fig. 7. The resolving powers are ~1000 at near 40 eV and over 700 at the *K* emission line of Li. Also they tend to decrease with increasing energy. It is thought that steep decrease in the higher energy side comes from Stark broadening of the source. In conclusion, the design value of the resolving power has been achieved for all the gratings (see Fig. 3).

5. *K*-emission spectrum of Li measured by TEM-SXES

A TEM-SXES experiment was demonstrated by a flat-field spectrograph equipped with the LR grating, which was attached to a TEM (JEM2010, JEOL Ltd.) at Tohoku University. As a reflection mirror for sagittally focusing soft x-rays that deviate from the direction of the grating, a pair of gold coated nickel plates with a length of 140 mm along incoming beam direction was installed between the grating and a specimen (light source). As a detector, a CsI-coated two-stage microchannel-plate (MCP) optically coupled with a CCD detector was installed. An effective pixel size on the MCP surface was evaluated to be a 24-μm in diameter. An electron beam size on the specimen for SXES experiments was usually a few μm in diameter. Since the size was enough smaller than that of a pixel size of the detector, an irradiated specimen area was considered as a point source for the spectrograph. Hence an entrance slit usually used in a soft x-ray spectrograph was unnecessary for TEM-SXES.

A fragment of metallic-lithium was mounted on a specimen holder in the argon atmosphere and transferred to the TEM chamber without exposing the specimen to the atmosphere, although the surface oxidation condition has not been checked in this experiment. Figure 8 shows the *K* emission spectrum of metallic lithium obtained under the condition of an acceleration voltage of 100 kV, an irradiation beam current of 13 nA, and an acquisition time of 5 min. A pressure in the specimen chamber of the TEM was about 1×10^{-5} Pa during the measurement. The intensity maximum placed at 54.1 eV with the full width at half maximum (FWHM) of 1.5 eV. The asymmetric intensity profile should be due to the DOS of VB of metal-Li, which agrees qualitatively well with previous literature[17, 18]. Also the background was suppressed to very low level. As presented above, other gratings of LM, BM, and BR are also expected to be comparable in efficiency, resolution, sensitivity, and background for obtaining the *K*-emission spectrum of lithium.

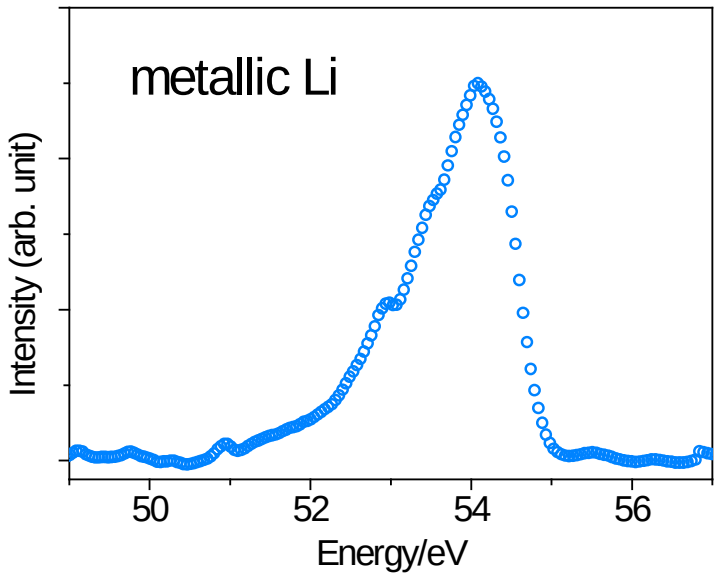

Fig. 8. *K* emission spectrum of metallic Li measured by TEM-SXES.

6. Summary

The purpose of this study is to develop a versatile flat-field spectrograph for the 50-4000 eV range to be attached to conventional EM's. Four holographic VLS gratings optimized for the respective energy ranges of 50-200 eV, 155-350 eV, 300-2200 eV, and 2000-4000 eV were designed. The laminar and blazed types gratings for the measurement of the *K* emission spectrum of lithium, which cover the lowest energy range of 50-200 eV and has an effective grating constant of 1/1200 mm, were fabricated with the aspheric wavefront recording system that made it possible to correct aberrations sufficiently. We fabricated four types of gratings, i.e., laminar and blazed types master and the respective replica gratings. They were evaluated on the absolute diffraction efficiencies and the resolving power using SR and LPP light sources, respectively. As the results, the diffraction efficiencies of the first order lights for the laminar type gratings (or blazed type gratings) are in excess of 5% (or 10%) at near 50 eV. In addition, the resolving powers of all gratings were evaluated to be over 700. The master and replica gratings showed comparable performance, and it is concluded that they can be practically used for TEM-SXES and other studies.

Acknowledgements

This work was conducted as a project of Collaborative Development of Innovative Seeds (Practicability verification stage) by Japan Science and Technology Agency.

References

1. M. Terauchi, H. Yamamoto and M. Tanaka, J. Electro. Microsc. 50, 101-104 (2001).
2. N. Nakano, H. Kuroda, T. Kita, and T. Harada, Appl. Opt. 23, 2386–2392 (1984).
3. M. Terauchi, M. Koike, K. Fukushima, and A. Kimura, J. Electr. Microsc. 59, 251-261 (2010).
4. T. Imazono, M. Ishino, M. Koike, H. Sasai, and K. Sano, Appl. Opt. 46, 7054-7060 (2007).
5. M. Koike, M. Ishino, T. Imazono, K. Sano, H. Sasai, M. Hatayama, H. Takenaka, P. A. Heimann, and E. M. Gullikson, Spectrochimica Acta B 64, 756–760 (2009).
6. T. Imazono, M. Koike, and M. Terauchi, H. Takahashi, and H. Sasai, Japanese patent pending.
7. T. Imazono, M. Koike, M. Koeda, T. Nagano, H. Sasai, Y. Oue, Z. Yonezawa, S. Kuramoto, M. Terauchi, H. Takahashi, N. Handa, and T. Murano, Proceedings of 21st Int'l Congress on X-ray Optics and Microanalysis (ICXOM21), AIP-CP (in press).
8. T. Namioka and M. Koike, Appl. Opt. 34, 2180−2186 (1995).

9. M. Koike, T. Namioka, E. Gullikson, Y. Harada, S. Ishikawa, T. Imazono, S. Mrowka, N. Miyata, M. Yanagihara, J. H. Underwood, K. Sano, T. Ogiwara, O. Yoda, and S. Nagai, Proc. SPIE, 4146, 163-170 (2000).
10. M. Koike and T. Namioka, Appl. Opt. 33, 2048−2056 (1994).
11. M. Koike, K. Sano, O. Yoda, Y. Harada, M. Ishino, N. Moriya, H. Sasai, H. Takenaka, E. Gullikson, S. Mrowka, M. Jinno, Y. Ueno, J. H. Underwood, and T. Namioka, Rev. Sci. Instrum. 73, 1541-1544 (2002).
12. H. Iwasaki, Y. Nakayama, K. Ozutsumi, Y. Yamamoto, Y. Tokunaga, H. Saisho, T. Matsubara, and S. Ikeda, J. Synchr. Radiat. 5, 1162-1165 (1998).
13. M. Koike and T. Namioka, Appl. Opt. 36, 6308-6318 (1997).
14. M. Koike and T. Namioka, Appl. Opt. 41, 245-257 (2002).
15. S. Bashkin and J. O. Stoner, Jr., *Atomic energy levels and Grotrian diagrams* (North-Holland Pub. Co., New York, 1975), Vol. 1, p. 12.
16. B. L. Henke, E. M. Gullikson, and J. C. Davis, At. Data Nucl. Data Tab. 54, 181-342 (1993).
17. O. Aita and T. Sagawa, J. Phys. Soc. Jpn. 27, 164-175 (1969).
18. S. Fukushima, T. Kimura, T. Ogiwara, and K. Tsukamoto, Microchim. Acta 61, 399-404 (2008).